Resonance Lines in Astrophysics

Manuscripts presented at a
Conference held in Boulder, Colorado
9-11 September 1968

December 1968

NATIONAL CENTER FOR ATMOSPHERIC RESEARCH
Boulder, Colorado

CONTENTS

J. L. Linsky

TOWARDS A SELF-CONSISTENT INTERPRETATION OF THE CALCIUM LINES

TOWARDS A SELF-CONSISTENT INTERPRETATION OF THE CALCIUM LINES

Jeffrey L. Linsky
Joint Institute for Laboratory Astrophysics*
Boulder, Colorado

ABSTRACT

From observations of the Ca II H and K resonance lines and subordinate infrared triplet we infer the behavior of the corresponding line source functions. These in turn are interpreted by means of four archetypal solutions of the statistical equilibrium and radiative transfer equations for the lines. Eclipse observations and continuum flux measurements in the ultraviolet and infrared place constraints upon acceptable solutions for the calcium lines. In the light of these constraints we consider several potential explanations for the 4200°K brightness temperature in K_1 and limb darkening of the entire profiles of H and K.

---

*of the National Bureau of Standards and University of Colorado.

I. INTRODUCTION

The Ca II H and K lines are unique in the solar visible spectrum as their doubly reversed profiles bear direct evidence of a chromospheric increase in temperature. As a result of their chromospheric dependence and the convenience of their being observable below the terrestrial atmosphere, these lines have been used to infer the physical properties and structure of the low chromosphere. Numerous analyses along these lines now exist (Miyamoto 1953, 1954, 1957; Jefferies and Thomas 1960; Athay and Skumanich 1968a, 1968b; Dumont 1967a, 1967b, 1968; Linsky 1968a*; Avrett and Linsky 1968; and Beebee and Johnson 1968), but each fails to explain some crucial observations or ignores some important aspect of the problem. Moreover, the calcium lines are usually analyzed independently of information on the chromosphere which has been gleaned from eclipse observations, measurements of continuum flux in the ultraviolet and infrared, and analyses of other lines. The net result is confusion to the extent that the calcium lines are now considered unreliable indicators of chromospheric properties.

In this paper we will attempt to clarify the nature of these lines by considering the data, the information they contain about the behavior of the line source functions, and the limitations on possible solutions for the line source functions imposed by other data on the chromosphere. We consider first four archetypal solutions to develop some insight into the sensitivity of the emergent line profiles to changes in the temperature structure and electron density distribution in the chromosphere. Next we summarize the data on the H and K lines as well as the subordinate infrared triplet. Finally we consider a number of possible means of satisfying the calcium

---

*Hereafter called Paper I.

line data within the limitations imposed by other data on the chromosphere. We hope that this approach will suggest the proper means of explaining these complex lines.

II. ARCHETYPAL SOLUTIONS FOR THE CALCIUM LINES

The aim of our analysis of the calcium lines is to infer the physical properties of the chromosphere; that is, the variation of electron temperature T_e, pressure P, densities, and nonthermal broadening parameters with height or reference optical depth. A complete specification of these properties constitutes a model. The chromosphere is generally taken to be plane-parallel and homogeneous at each height, although two component models (Beebee and Johnson 1968) have now been considered. In computing a model we find (Paper I) that by assuming hydrostatic equilibrium and detailed balance in the Lyman lines of hydrogen, we need only specify a photospheric density or optical depth, and the variation with height of T_e and the nonthermal broadening, given in terms of an equivalent nonthermal velocity.

After constructing a model we next solve statistical equilibrium equations for the lower and upper levels of all relevant transitions together with the radiative transfer equations for these transitions to obtain the line source functions S. From these we compute the emergent specific intensities $I_\nu(\mu)$, where μ is the usual cosine of the normal angle and ν is the frequency. For details of our method of solving the source function equations and calcium ionization equilibria we refer the reader to Paper I. We mention only that the ionization equilibria are given by solutions of the relevant statistical equilibrium equations, and that the source function equations are solved in the kernel approximation as described by Avrett and

Loeser (1966). The four solutions which we will describe assume complete redistribution in frequency for the scattering process and chromospheric models in hydrostatic equilibrium. We consider a 3 level Ca II ion consisting of the 4 $^2S_{1/2}$ ground state, 3 $^2D_{5/2}$ and 4 $^2P_{3/2}$ excited states and a continuum. The 4 $^2P_{3/2} \rightarrow$ 4 $^2S_{1/2}$ transition is the K line at 3933 Å and the 4 $^2P_{3/2} \rightarrow$ 3 $^2D_{5/2}$ transition is the infrared triplet line at 8542 Å. The 4 $^2P_{1/2}$ and 3 $^2D_{3/2}$ levels are irrelevant (Paper I) and higher lying levels have not been considered.

Model A results from a straight forward attempt to match the observed low spatial resolution K line profile (White and Suemoto 1968) at the center of the solar disk. The temperature distribution as shown in Fig. 1 has a narrow minimum of 4200 °K centered near 500 km*, followed by a slow rise in temperature and then a much steeper rise beginning at 1300 km. The resultant electron density distribution (see Fig. 2) has a relative maximum of 1.4×10^{11} at 1500 km, where hydrogen is fully ionized. The assumption of a nonthermal velocity distribution with a maximum value of 4.5 km/sec (see Fig. 3) results in an emergent K line profile, shown in Fig. 4, which is in qualitative agreement with the data. In particular the profile has a doubly reversed shape consisting of a central absorption feature (K_3), a relative maximum (K_2) away from the core, and a relative minimum (K_1) in the inner wings.

The essential aspect of Model A is that K_1 is formed at roughly 10^5 line center optical depths. In general, a line source function saturates to the local Planck function at line center optical depths in excess of a thermalization length Λ. For a Voigt profile and a two-level atom $\Lambda \sim a\varepsilon^{-2}$

---

*Heights are given on the model atmospheres scale, that is above radial optical depth at 5000 Å of unity ($\tau_{5000} = 1$).

(Avrett and Hummer 1965), where a is the Voigt parameter, and ε (which is proportional to n_e) is essentially the probability per scattering with a Ca II ion that a line photon will be destroyed. Near 500 km in the sun (see Paper I) $\varepsilon \gtrsim 10^{-4}$ and $a \gtrsim 10^{-4}$ so that $\Lambda \gtrsim 10^{+4}$. Thus K_1 in this model is formed in a region where $S \gtrsim B$ and Model A would be considered "effectively thick," or in Jefferies' notation (Gingerich and De Jager 1968), "optically thick."

Models B and C are slight variants of Model A in which the temperature structure and nonthermal velocities are unchanged, but the mean molecular weights are altered to change the electron densities. We assume a helium to hydrogen number ratio of 0.05 for Model B and 0.20 for Model C instead of the more commonly accepted value of 0.10 used in Model A. These models serve to illustrate the effect of increasing the total and electron densities a factor of 3 in the case of Model B or decreasing them a factor of 10 in the case of Model C in the region where K_2 and K_3 are formed (see Fig. 2). As shown in Figs. 4 and 5, a factor of 3 increase in n_e decreases Λ and increases the coupling of S to B such that K_2 and K_3 are strongly enhanced. The profile now resembles that seen in a plage. On the other hand, an order of magnitude decrease in n_e lengthens Λ and thereby reduces the coupling of S to B. In this case the profile is a very deep absorption line with no K_2 feature.

These two models are not as artificial as they might appear for a number of mechanisms may alter the electron density where K_2 and K_3 are formed. For example, if the turbulent velocities are small compared to the sound velocity, then their effect will be to increase pressure scale heights without altering $T_e(h)$ and thus to mimic the qualitative behavior of Model B. Also, displacement in height of the temperature rise of Model A will simulate the behavior of Models B or C depending upon whether the displacement is inwards or outwards.

Model D is an attempt to produce a K line profile similar to that observed with a different form of temperature distribution. As suggested by considerations to be discussed later, the temperature minimum is raised to 4600 °K and extends from 300 km to 900 km. As thermalization occurs near 500 km the source function falls increasingly below the Planck function with height until a steep rise in B produces a relative maximum in S near 1500 km. The source function thus has a relative minimum at optical depths near 100, which maps into the K_1 feature, if we assume nonthermal velocities increasing to 11.4 km/sec. Since K_1 is formed at optical depths considerably less than Λ, this model may be classified as "effectively thin."

With these archetypal models in mind we now discuss the observations and the information they contain on the formation of the calcium lines.

III. OBSERVATIONS OF THE H AND K LINES

We wish to summarize some important aspects of the observational material for the calcium lines which are essential to an adequate interpretation of the lines. Data on the H and K lines can be divided into two distinct groups depending on whether they were obtained at low or at high spatial resolution on the solar disk. Only the former has been the subject of systematic investigation. Its basic features and their significance are, briefly:

(1) The line profiles have emission features called H_2 and K_2 on either side of the central absorption cores (H_3 and K_3) and inside secondary absorption features (H_1 and K_1) in the inner wings. If complete redistribution in frequency space is a valid description of the scattering process, as is usually presumed, this doubly reversed line shape requires a relative maximum and minimum in the frequency-independent line source functions in the low chromosphere.

(2) The entire profiles are known to limb darken, a behavior which is inconsistent with a relative maximum and minimum in a frequency-independent source function S unless the chromosphere is multicomponent (Avrett and Linsky 1968, Beebee and Johnson 1968) or the mapping of S onto the emergent specific intensity $I_\nu(o,\mu)$ is such that the relative minimum is masked at $\mu = 1$ but less so towards the limb (Athay and Skumanich 1968b).

(3) Outside of active regions, and except for limb darkening, the line profiles do not vary significantly from place to place on the disk (Teske 1967). This behavior lends some justification to a one-component model for the chromosphere.

(4) The brightness temperatures for H_1 and K_1 are roughly 4200°K. Thus the minimum values for the H and K line source functions cannot be larger than those of the corresponding Planck functions at 4200°K. If, as in the "effectively thick" model, H_1 and K_1 are formed at sufficiently large line center optical depths that the relative populations for their lower and upper levels are close to the LTE values, then the solar minimum temperature can be no larger than 4200°K. On the other hand, if the solar minimum

temperature is roughly 4600°K, then the 4 $^2P_{1/2}$ and 4 $^2P_{3/2}$ levels must be underpopulated relative to the ground state 4 $^2S_{1/2}$ where H_1 and K_1 are formed. This can only occur if H_1 and K_1 are formed at line center optical depths significantly less than a thermalization length, as in the "optically thin" model, or if complete redistribution is inaccurate in the line wings.

(5) Both of the resonance lines are slightly asymmetric about the rest wavelengths indicating a net systematic motion outward in the low chromosphere.

(6) The relative residual intensities in H_3 and K_3 are very nearly equal. This equality results from coupling of the 4 $^2P_{1/2}$ and 4 $^2P_{3/2}$ levels via collisions and transitions with the 3 ^2D levels (Linsky 1968b, 1968c).

(7) The profiles undergo a systematic but gradual transition from regions of the "quiet" chromosphere to plages (see Sheeley 1967). The changes are not qualitative, for the profiles retain their doubly reversed shape, but rather quantitative with residual intensities in K_2 increasing from roughly 5% in "quiet" regions to roughly 30% in plages. This gradual transition suggests a gradual increase in $T_e(h)$ where K_2 and K_3 are formed, or in the coupling between the line source functions and the Planck function such as would occur with an increase in electron density as seen by comparing Model B to Model A.

(8) The cores of H and K are quite broad, roughly 0.34 Å between the K_2 peaks and 0.50 Å between the K_1 minima at the center of the disk according to the data of White and Suemoto (1968). The broadening mechanism is generally taken to be Doppler in the line cores, but the inferred halfwidths $\Delta\lambda_D$ depend upon the optical depth of formation of the K_2 and K_1 features. Goldberg (1957) showed that for constant $\Delta\lambda_D$, which is primarily turbulent, velocities

of 20 km/sec are required if the line center optical depth is very small where K_1 is formed, but only 5.5 km/sec if it is of order 10^5. Both theoretical (Athay and Skumanich 1968a) and empirical (Zirker 1968) considerations suggest that $\Delta\lambda_D$ increases outward. Nevertheless, Zirker finds that velocities of order 11 km/sec are required to place the K_2 peaks at their proper wavelengths if the source function relative maximum lies at optical depth of order 3.

These, then, are the essential aspects of an artificial set of H and K line data obtained by averaging over the observed fine structure. We defer until later the question of whether these mean data can yield properties of a meaningful mean chromosphere.

At high spatial resolution the H and K line profiles exhibit a different group of properties:

(1) Under conditions of excellent seeing, spectroheliograms in K_3 and $K_2 + K_3$ reveal structure at the limit of spatial resolution, less than 500 km in width. This scale corresponds to line center optical depths of 5 and 1000 in K_3 and K_2, respectively, for Model A. In the "effectively thin" Model D, corresponding values are 4 and 20. As the thermalization lengths are of order 10^4, these data suggest that the radiative transfer equations for these lines ought to be solved in a three-dimensional medium rather than in one dimension.

(2) In spectroheliograms taken in K_3 or $K_2 + K_3$, supergranule cells appear as dark regions and the intercellular network or "coarse network" and plage regions are bright. As first shown by Babcock and Babcock (1955) there is a positive correlation of bright H and K emission with regions of

large magnetic field. Zirin (1966) points out that the increase in magnetic field from the interior of a supergranule to the network is sufficient to make the magnetic energy density dominant over the kinetic energy density in the network but insignificant compared to the kinetic energy density in supergranules. This qualitative difference suggests that one consider an idealized two-component chromosphere. Since the strength of the emission feature increases with electron density and with a displacement of the steep temperature rise inward, there appears to be a correlation of large magnetic fields with either or both of these changes. In view of the enhanced magnetic fields and brighter K_2 emission in plages, it is tantalizing to suggest that plage regions are similar but enhanced versions of physical conditions in the "coarse network."

(3) Zirin (1966) states that "under the scrutiny of high spatial and spectroscopic resolution the myth of doubly reversed emission lines falls." By this he means that under high resolution the profile rarely if ever has a doubly reversed shape, but rather has an irregular dark core surrounded by some patches of emission. Displacements in wavelengths of these features with position on the disk suggest large systematic motions in the vertical direction. From the lateral scale of profile variations discussed above, many distinct regions with different systematic motions ought to exist within a radius of one local thermalization length at heights where the cores are formed. Consequently, the assumption of microturbulent velocity fields could be valid, in which case the fitting of computed profiles to the low spatial resolution data has physical meaning. To date there exist few theoretical investigations

of line formation in a differentially moving atmosphere and none where the scale of variation of such motions is small enough to suggest microturbulence. This latter case deserves treatment and the high spatial resolution H and K profiles may provide a test example.

IV. OBSERVATIONS OF THE CALCIUM INFRARED TRIPLET

Coupled to the H and K lines are three lines in the infrared at 8498, 8542, and 8662 Å with the same upper levels $4\ ^2P_{1/2}$ and $4\ ^2P_{3/2}$ as the H and K lines but with metastable lower levels $3\ ^2D_{3/2}$ and $3\ ^2D_{5/2}$. These lines appear qualitatively different from the H and K lines over most of the disk, yet their theoretical interpretation involves the solution of the same set of statistical equilibrium equations as for the H and K lines and the same assumptions in solving the radiative transfer equations. The lines, therefore, contain additional information on the chromosphere and provide additional constraints upon acceptable chromospheric models. Because the paucity of data on spatial resolution, we discuss only the lower resolution work of De Jager and Neven (1967) and of Linsky and Wilkinson (1968).

(1) Profiles of the infrared lines, unlike the H and K lines, exhibit no emission features. This suggests that the line source functions decrease monotonically with height over the region of line formation, and that they do not reflect a chromospheric rise in temperature. This insensitivity to the temperature rise results from the small line center optical depth at which it occurs.

(2) Each of the infrared lines limb darken, a natural consequence of source functions which decrease monotonically with height.

(3) The sequence of increasing opacity in the 8498, 8662, and 8542 Å lines is also a sequence of decreasing central residual intensity, although

the data are ambiguous concerning the 8662 and 8542 Å lines. We find that at a level where $\tau_{8542} \approx 1$, opacities in the three lines are typically 0.018, 0.009, and 0.0019 compared to that of the K line. At this depth in the chromosphere densities are sufficiently high that collisions between the $4\ ^2P_{1/2}$ and $4\ ^2P_{3/2}$ levels insure equilibrium relative to populations in the two levels (Paper I). Presumably the same is also true for the $3\ ^2D_{3/2}$ and $3\ ^2D_{5/2}$ levels. Consequently, the source functions for the three lines should be essentially equal at the same position in the chromosphere. This deduction, together with the monotonic behavior of the source functions deduced above, accounts for the relative strength of the lines.

(4) Central residual intensities for the two strongest lines are observed to be roughly 0.18 while that of the 8498 Å line is 0.26 to 0.30. These data may be compared with theoretical intensities of our four models in Fig. 6. Both Models A and D predict intensities of roughly 0.07 for the two strong lines and 0.12 for the 8498 Å line, in disagreement with observations. One way of bringing about better agreement would be to reduce Λ by increasing the electron densities near 1000 km where the cores of the lines are formed. As we shall mention in the next section, this change will bring the electron densities into better agreement with the eclipse data.

(5) Spectroheliograms in the cores of the infrared lines as for example those of Title (1967) reveal a bright coarse network and plages similar in detail to that seen in H and K, although the contrast between bright and dark regions is significantly smaller than for H and K. Evans and Michard (1962) measure root-mean-square intensity fluctuations in the core of the 8542 Å line of 0.118, whereas a corresponding value for K_3 would be greater than unity as shown by the Jensen and Orrall (1963) data. This similarity with

H and K makes sense because any mechanism, such as an increase in electron density, which more closely couples a line source function to a steeply rising local Planck function in the chromosphere affects both resonance and subordinate lines as shown in Figs. 4 and 6.

(6) In plages the infrared lines acquire emission features and a doubly reversed profile like the H and K lines. Mustel and Tsap (1958) observed residual intensities of roughly 0.60 for the IR_2 features (analogous to H_2 and K_2), considerably in excess of values for quiet regions of the disk. These data confirm the suggestion made above that plage regions are regions of higher density and thus closer coupling to local conditions than the surrounding medium.

V. CHROMOSPHERIC BOUNDARY CONDITIONS

We turn our attention now to limitations upon possible explanations of the calcium lines imposed by observations of continuum flux and other lines found in the chromosphere.

(1) Considerable empirical evidence points towards a minimum temperature at the base of the solar chromosphere of roughly 4600°K. As summarized in Gingerich and De Jager (1968) and Paper I, these arguments consist primarily of interpretations of the continuum flux near 1600 Å, carbon monoxide abundance, and silicon opacity discontinuities. Each of these arguments presumes a one-component chromosphere, whereas the calcium lines suggest two components. In a two-component medium the mean temperature may not be the same as that deduced from averaged continuum observations assuming a one-component chromosphere. Indeed, Brown and Linsky (1968) argue that the mean temperature will be less than that deduced for a one-component model and that a mean

temperature of 4200°K could be consistent with the continuum flux near 1600 Å if root-mean-square thermal fluctuations are as large as 500°K. Although we predicate our ensuing analysis upon the assumption of a 4600 °K temperature minimum, we wish to point out that the assumption may be wrong and a plausible mechanism exists for its being wrong.

(2) Interpretations of continuum and hydrogen line observations obtained during an eclipse provide some information on physical properties of the low chromosphere. These data are generally given in terms of an eclipse height scale where height zero is defined by the relation $d^3E_\lambda/dh^3 = 0$ with E_λ the observed intensity of radiation in the continuum at a standard wavelength such as 5000 Å. In an isothermal atmosphere height zero corresponds to $\tau_\lambda(\text{tang}) = 1$. We transform eclipse heights to the model atmospheres height scale by adding 300 km, obtained using the Bilderberg continuum atmosphere (Gingerich and De Jager 1968) and $\lambda = 4700$ Å. This change in height zero is subject to the uncertainties associated with the BCA.

Thomas and Athay (1961) obtained a chromospheric model above 1050 km from continuum data at 3646 Å and 4700 Å. In deriving the model they assumed hydrostatic equilibrium and employed solutions for a three-level hydrogen atom. Their derived temperatures and electron densities are given in Figs. 1 and 2. Below 800 km their data are too noisy to derive a unique model, so instead they extrapolate inwards assuming hydrostatic equilibrium and some continuum data. The resultant thermodynamic quantities are also given, but the authors expect that below 800 km the model represents an upper bound upon the electron temperature.

Two other eclipses provide additional information on the chromosphere. The 1962 eclipse data as described by Henze (1968) differ somewhat from the

1952 data. The 1962 data yield no unique model but instead a family of models derived from the high Balmer and Paschen lines assuming hydrostatic equilibrium. Electron densities for these models, which fall within a narrow range, are given in Fig. 2 and are roughly a factor of two lower than the Thomas-Athay values. The data of the 1966 eclipse as interpreted by Weart (1968) have increased height resolution, taking into account the irregular edge of the moon. These data yield emission scale heights in the low chromosphere (< 800 km) as low as 50 km, which Weart finds explicable only by H^- emission at temperatures lower than 5000°K. The data thus imply that over the extended region of 300-800 km on the model atmospheres height scale there is a flat temperature minimum with $T_e \leq 5000$°K. This result is evidence for our "effectively thin" Model D.

(3) With respect to the eclipse data we should mention that in a static atmosphere the thermodynamic state variables of pressure, temperature, and density may not be chosen independently, but are related by the perfect gas law and by the condition of hydrostatic equilibrium. The chromosphere, however, is neither a static nor a homogeneous medium. Clearly, when constructing a model for the chromosphere or one component of it, one would like to incorporate dynamic equilibrium considerations into the model. In Paper I we have computed models with a "turbulent pressure" term in the hydrostatic equilibrium equation, but a more meaningful representation of what should be called hydrodynamic equilibrium is one of the outstanding problems of the chromosphere.

(4) In the upper photosphere and low chromosphere the speed of sound increases with height from roughly 6.5 to 11.5 km/sec. Small scale turbulent velocity fields much in excess of this value suggest shocks of such strength that they would be immediately damped by a large dissipation of energy.

Random motions as large as 10-15 km/sec are required to match the H and K profiles, however, when the emission peaks are found at optical depths of order 10 as required by "effectively thin" models. This argument would be a strong one against "thin" models if we understood the nature of these random motions.

VI. EXPLANATIONS FOR A K_1 BRIGHTNESS TEMPERATURE OF 4200°K WITH A 4600°K TEMPERATURE MINIMUM

As suggested above the solar minimum temperature and the extent of the minimum region play a crucial role in interpreting the H and K line profiles. If the minimum region is relatively narrow as in Model A, then K_1 is formed there and the brightness temperature in K_1 cannot be less than the solar minimum temperature. This "effectively thick" model requires a minimum temperature no higher than 4200°K which we have ruled out. Assuming a minimum temperature of 4600°K, we consider the following explanations of the K_1 feature.

(1) Most analyses of resonance lines assume complete distribution in frequency space during the scattering of a photon. This assumption is valid in the line core due to thermal motions of the scattering particle (Thomas 1957), but is not valid in the wings if radiation damping dominates over collisional broadening of the upper level of the transition involved (Zanstra 1941, Holstein 1947). In the sun radiation damping dominates over collisional broadening for the H and K lines and also over collisional transitions between the 4 $^2P_{1/2}$ and 4 $^2P_{3/2}$ levels above 400 km (Paper I), so that coherent scattering in the <u>rest frame</u> of the Ca II ion is a good approximation.

Jefferies and White (1960) and Avery and House (1968) show that under these conditions Doppler motions only slightly rearrange the frequency of wing photons, that is those beyond 3 Doppler halfwidths from line center. Therefore complete redistribution in the observer's frame of reference is probably not valid in the wings, although there remains some uncertainty about the role played by collisions in the redistribution process (Edmonds 1955).

The effect of partial coherency in the wings is to make the source function frequency-dependent and to depress the emergent profile in the wings below that for the complete redistribution case. In physical terms the effect of coherency is to force the monochromatic source function to thermalize at monochromatic optical depths in excess of $\Lambda = \varepsilon^{-1/2}$, instead of at line center optical depths in excess of $\Lambda = a\varepsilon^{-2}$. Since monochromatic optical depths in the wings can be many orders of magnitude less than at line center, the possibility exists that the inner wings (including K_1) can be less saturated than the outer core (including K_2) for which complete redistribution is valid. In fact, Jefferies and White (1960) and Hummer (1968) find that this mechanism can form a doubly reversed profile even in an isothermal atmosphere. Computations are now underway for the H and K lines incorporating partial coherency in the wings and we expect the mechanism to decrease K_1 relative to the temperature minimum value. If this mechanism is the correct explanation of the K_1 feature, then it should also tend to reduce the discrepancy between the eclipse electron densities near 1000 km and those of Models A and D (see Fig. 2). This would occur because Λ could be smaller, and thus ε and n_e larger, due to the reduced saturation in the inner wings.

(2) A second possible mechanism* for decreasing the intensity of K_1 relative to the solar minimum temperature concerns the influence of the 3 ^2D levels upon the population of 4 $^2P_{3/2}$. For simplicity we consider only the 3 $^2D_{5/2}$ level labeled 2, the 4 $^2P_{3/2}$ level labeled 4, and the ground state 4 $^2S_{1/2}$ labeled 1. From the statistical equilibrium equation for these levels and the radiative transfer equation we obtain for the K line (4 → 1) source function

$$S_{41} = \frac{\bar{J}_{41} + \tilde{\varepsilon}_{41}\tilde{B}_{41}}{1 + \tilde{\varepsilon}_{41}} , \qquad (1)$$

where $\bar{J}$ is the integrated line intensity and

$$\tilde{\varepsilon}_{41} = \frac{C_{41}}{A_{41}} \left[1 + \frac{NCR_{42} + NRR_{42}}{C_{41}}\right] \qquad (2)$$

$$\tilde{B}_{41} = \frac{B_{41}}{1 + \left(\frac{NCR_{42} + NRR_{42}}{C_{41}}\right)} . \qquad (3)$$

In these equations B_{41} is the local Planck function, C_{ij} and A_{ij} are collisional and radiative de-excitation rates, and NCR_{42} is the net collisional rate from level 4 to level 2 defined as

$$NCR_{42} = C_{42} - \frac{n_2}{n_4} C_{24} = C_{42} \left(1 - \frac{b_2}{b_4}\right) \qquad (4)$$

with n_i and b_i the population and departure coefficient for level i.

---

*We wish to thank Dr. E. Avrett for first pointing out this effect.

Also NRR_{42} is the net radiative rate from level 4 to level 2 defined by

$$NRR_{42} = A_{42} + B_{42}\,\bar{J}_{42} - \frac{n_2}{n_4}\,B_{24}\,\bar{J}_{42} = A_{42}\,\rho_{42} \quad , \qquad (5)$$

where B_{42} and B_{24} are the usual Einstein coefficients of stimulated emission and absorption, and ρ_{42} is the net radiative bracket. The sum $NCR_{42} + NRR_{42}$ represents the net depopulation rate of the 4 $^2P_{3/2}$ level due to the inclusion of the 3 $^2D_{5/2}$ level.

At optical depths which are large compared to the thermalization lengths of the K and infrared lines, $\rho_{42} = 0$ and $b_2/b_4 = 1$; that is, the 4 $^2P_{3/2}$ and 3 $^2D_{5/2}$ levels are in equilibrium. At smaller optical depths we find that for both "thin" and "thick" models the first departures from LTE are in the direction $\rho_{42} > 0$ and $b_2/b_4 > 1$. We plot in Fig. 7 the ratio of $NCR_{42} + NRR_{42}$ to C_{41} for Models A and D. For the thick model K_1 is formed at larger optical depths than a thermalization length in a region where $(NCR_{42} + NRR_{42})/C_{41}$ is slightly negative. Thus $\tilde{B}_{41} > B_{41}$ and the K line source function is approximating $\tilde{B}_{41}$. As a result, the inclusion of the 3 $^2D_{5/2}$ level tends to raise rather than lower the intensity of K_1. Skumanich (1968) also finds the inclusion of the 3 $^2D_{5/2}$ level does not decrease K_1. For the "optically thin" model K_1 is formed at small optical depths so that the driving term $\tilde{\varepsilon}_{41}\,\tilde{B}_{41}$ in Eq. 1 rather than the generalized Planck function $\tilde{B}_{41}$ is significant. Since $\tilde{\varepsilon}_{41}\tilde{B}_{41} = C_{41}B_{41}/A_{41}$ is unaffected by the 3 $^2D_{5/2}$ level, K_1 is also unaffected by it.

(3) A third potential means of explaining the intensity of K_1 is by means of the "effectively thin" model (Model D). The essential aspect of

this model, namely an extended temperature minimum, is suggested by Curtis and Jefferies' (1967) analysis of the Na D lines, Weart's (1968) analysis of the 1966 eclipse data, and by the 22.5μ, 24.3μ, and 1.2 mm limb darkening data of Noyes, Beckers, and Low (1968). The model does pose some problems, however, in that it requires large nonthermal random velocities and electron densities considerably less than the eclipse data warrant.

(4) A final point we might mention is that systematic velocity gradients in both the vertical and the horizontal directions tend to reduce saturation and thus reduce the local source function. The effect of velocity gradients in the line of sight has been investigated by Hummer and Rybicki (1968). Horizontal gradients have not been investigated, but they should reduce saturation by allowing the lateral escape of photons in the line core into a moving medium where the photons are now in the line wings. Both effects work in the direction of lowering K_1 relative to the temperature minimum value. Since microturbulence cannot simulate these effects of systematic velocity gradients, models of a mean chromosphere which yield profiles in agreement with the low spatial resolution data may bear only slight resemblance to actual chromospheric conditions.

VII. POSSIBLE EXPLANATIONS FOR LIMB DARKENING

Perhaps the most significant aspect of the low spatial resolution data, as shown by White and Suemoto (1968) and by Zirker (1968), is that the entire profiles of the H and K lines limb darken. As mentioned earlier the doubly reversed H and K line shapes require line source functions which have a relative maximum and a relative minimum in the chromosphere. This property in turn appears to be difficult to reconcile with limb darkening in K_1 and K_2. We mention two possible explanations of this limb darkening.

(1) Athay and Skumanich (1968b) propose to explain limb darkening throughout the line cores by an "effectively thick" model in which the nonthermal velocity increases with height in the region of the source function relative maximum. This approach gives the right qualitative behavior. However, since their model is "effectively thick" the source function minimum is masked at $\mu = 1$ and the resultant minimum temperature is 4000°K. This temperature appears to us to be quite implausible, but if it is raised to 4600°K no "effectively thick" model can explain the observed intensity of K_1. Thus we search for alternative solutions.

(2) Avrett and Linsky (1968) suggest that a two component model may explain limb darkening. This model is based upon the appearance of bright and dark regions in spectroheliograms and the correlation of these features with supergranule cells and the intercellular network mentioned previously. In this model the line source functions in dark regions decrease monotonically with height as in Model C, while in bright regions the source functions have a pronounced emission feature as in Model B. The resultant line profiles in the dark region will limb darken, whereas the K_1 and K_2 features for the bright region will not. The combined profile should thus have the same qualitative behavior as the data. This mechanism should also work for "effectively thin" models where the difference in the individual line profiles could either be due to variations in the electron density or to the placement of the steep temperature rise. Calculations along these lines are now underway.

There are two obvious checks upon the suitability of this mechanism for explaining limb darkening. First, plages contain few, if any, dark regions yet the entire cores of H and K limb darken (Smith 1960). Thus some other mechanism must be responsible for the limb darkening in plages. Second, high spatial resolution spectrograms resolve individual bright and dark regions and thus provide a direct check. Such spectrograms as in Zirin (1966) do show alternating profiles with weak and strong K_2 emission patches, but the spectrograms are not calibrated to allow a more detailed comparison of typical dark and bright profiles. We would not be surprised if both mechanisms herein described are necessary to account for limb darkening in quiet regions of the chromosphere.

VIII. CONCLUSIONS

In this paper we have sought to explain the essential aspects of the calcium lines as inferred from the observed line profiles in terms of solutions of the radiative transfer and statistical equilibrium equations consistent with other data on the chromosphere. We conclude by mentioning three outstanding problems whose solutions should greatly clarify our understanding of the formation of these lines. First, we would like to see solutions of the radiative transfer equation in three dimensions so as to interpret the observed small scale structure and profiles in terms of local physical conditions. Such solutions incorporating systematic motions ought to clarify the meaning of the large nonthermal motions necessary to reproduce the observed low spatial resolution profiles. Second, the two potential explanations for limb darkening ought to be investigated in more detail to determine which is the more important cause of limb darkening. Finally, the computed central intensities of the infrared lines appear to be a factor of 3 too low and the inferred electron densities near 1000 km appear to be nearly an order of magnitude too low. These discrepancies suggest that we may be ignoring an important detail in the formation of the calcium lines as, for example, partial coherency in the line wings which should have the effect of increasing n_e where the cores of the infrared lines are formed and thus increasing their central intensities.

ACKNOWLEDGMENT

This paper has been immeasurably aided by discussions with many colleagues. In particular, we would like to thank Drs. E. Avrett, R. N. Thomas, and D. Hummer for their assistance. The work was supported by National Aeronautics and Space Administration through a grant to the University of Colorado. NGR-06-003-057

REFERENCES

Athay, R. G. and Skumanich, A. 1968a, Solar Phys., 3, 181.

Athay, R. G. and Skumanich, A. 1968b, Solar Phys., 4, 176.

Avery, L. W. and House, L. L. 1968, Astrophys. J., 152, 493.

Avrett, E. H. and Hummer, D. G. 1965, Mon. Not. Roy. Astron. Soc. 130, 295.

Avrett, E. H. and Linsky, J. L. 1968, Astron. J., 73, S54.

Avrett, E. H. and Loeser, R. 1966, Smithsonian Special Report, 201.

Babcock, H. W. and Babcock, H. E. 1955, Astrophys. J., 121, 349.

Beebee, H. A. and Johnson, H. R. 1968, this volume.

Brown, D. R. and Linsky, J. L. 1968, to be published.

Curtis, G. W. and Jefferies, J. T. 1967, Astrophys. J., 150, 1061.

De Jager, C. and Neven, L. 1967, Bull. Astron. Inst. Neth., Suppl. Series, 1, 325.

Dumont, S. 1967a, Ann. Astrophys., 30, 421.

Dumont, S. 1967b, Ann. Astrophys., 30, 861.

Dumont, S. 1968, Ann. Astrophys., 31, 101.

Edmonds, F. N. 1955, Astrophys. J., 121, 418.

Evans, J. W. and Michard, R. 1962, Astrophys. J., 136, 487.

Gingerich, O. and De Jager, C. 1968, Solar Phys., 3, 5.

Goldberg, L. 1957, Astrophys. J., 126, 318.

Henze, W. Jr. 1968, "Chromospheric hydrogen spectrum at the 1962 Solar Eclipse," NCAR cooperative thesis No. 11.

Holstein, T. 1947, Phys. Rev., 72, 1212.

Hummer, D. G. 1968, private communication.

Hummer, D. G. and Rybicki, G. 1968, this volume.

Jefferies, J. T. and Thomas, R. N. 1960, Astrophys. J., 131, 695.

Jefferies, J. T. and White, O. R. 1960, Astrophys. J., 132, 767.

Jensen, E. and Orrall, F. Q. 1963, Astrophys. J., 138, 252.

Linsky, J. L. 1968a, Smithsonian Special Report, 274.

Linsky, J. L. 1968b, Astron. J., 73, S68.

Linsky, J. L. 1968c, to be published.

Linsky, J. L. and Wilkinson, C. W. 1968, to be published.

Miyamoto, S. 1953, Z. Astrophys., 31, 282.

Miyamoto, S. 1954, Publ. Astron. Soc. Japan, 6, 196.

Miyamoto, S. 1957, Publ. Astron. Soc. Japan, 9, 146.

Mustel, E. P. and Tsap, T. T. 1958, Izvestia Krimskoy Astrofizicheskoy Observatorii, 20, 74.

Noyes, R. W., Beckers, J. M., and Low, F. J. 1968, Solar Phys., 3, 36.

Sheeley, N. R., Jr. 1967, Astrophys. J., 147, 1106.

Skumanich, A. 1968, private communication.

Smith, E. 1960, Astrophys. J., 132, 202.

Teske, R. G. 1967, Publ. Astron. Soc. Pacific, 79, 110.

Thomas, R. N. 1957, Astrophys. J., 125, 260.

Thomas, R. N. and Athay, R. G. 1961, Physics of the Solar Chromosphere, Interscience, New York.

Title, A. 1967, Selected Spectroheliograms, Mount Wilson and Polomar Observatories, Pasadena.

Weart, S. R. 1968, "Photoelectric eclipse observations of continuum and coronal line emission at the solar limb," JILA Report No. 96, Joint Institute for Laboratory Astrophysics, Boulder, Colorado.

White, O. R. and Suemoto, Z. 1968, Solar Phys., **3**, 523.

Zanstra, H. 1941, Mon. Not. Roy. Astron. Soc., **101**, 273.

Zirin, H. 1966, The Solar Atmosphere, Blaisdell, Waltham, Mass.

Zirker, J. B. 1968, Solar Phys. **3**, 164.

FIGURE LEGENDS

Fig. 1. Temperature distribution of several proposed models of the solar chromosphere. Included are Models A, B, C, and D described in Section II, the Bilderberg Continuum Atmosphere (BCA), and the eclipse-based models of Weart (1968) and Thomas and Athay (1961). Arrows designate the corresponding distributions as upper limits, and heights are measured above radial $\tau_{5000} = 1$.

Fig. 2. Electron density distributions of several proposed models of the solar chromosphere. Included are Models A, B, C, and D described in Section II, the Bilderberg Continuum Atmosphere (BCA), and the eclipse-based models of Henze (1968) and Thomas and Athay (1961). Error bars on the Henze data refer to the maximum range of his data. Below 800 km the Thomas and Athay densities refer to the upper limit temperatures in Fig. 1.

Fig. 3. Nonthermal velocities assumed for the "effectively thick" Models A, B, and C, and for the "effectively thin" Model D.

Fig. 4. K line specific intensities at the center of the solar disk computed using Models A, B, C, and D are compared with the observed profile of White and Suemoto (1968).

Fig. 5. Local Planck functions and corresponding source functions for Models A, B, C, and D.

Fig. 6. Specific intensities for the 8542 Å line at the center of the solar disk computed using Models A, B, C, and D. Also given is the observed profile of Linsky and Wilkinson (1968).

Fig. 7. Plotted are the ratios of the net transition rate $4\ ^2P_{3/2} \rightarrow 3\ ^2D_{5/2}$ ($NCR_{42} + NRR_{42}$) compared to the downward collisional rate $4\ ^2P_{3/2} \rightarrow 4\ ^2S_{1/2}$ (C_{41}) for Models A and D. Included are optical depths in the 42 transition, position of thermalization of 42 photons, and the height where K_1 is formed for each model. The latter two positions are designated by arrows on the appropriate τ_{42} scales.

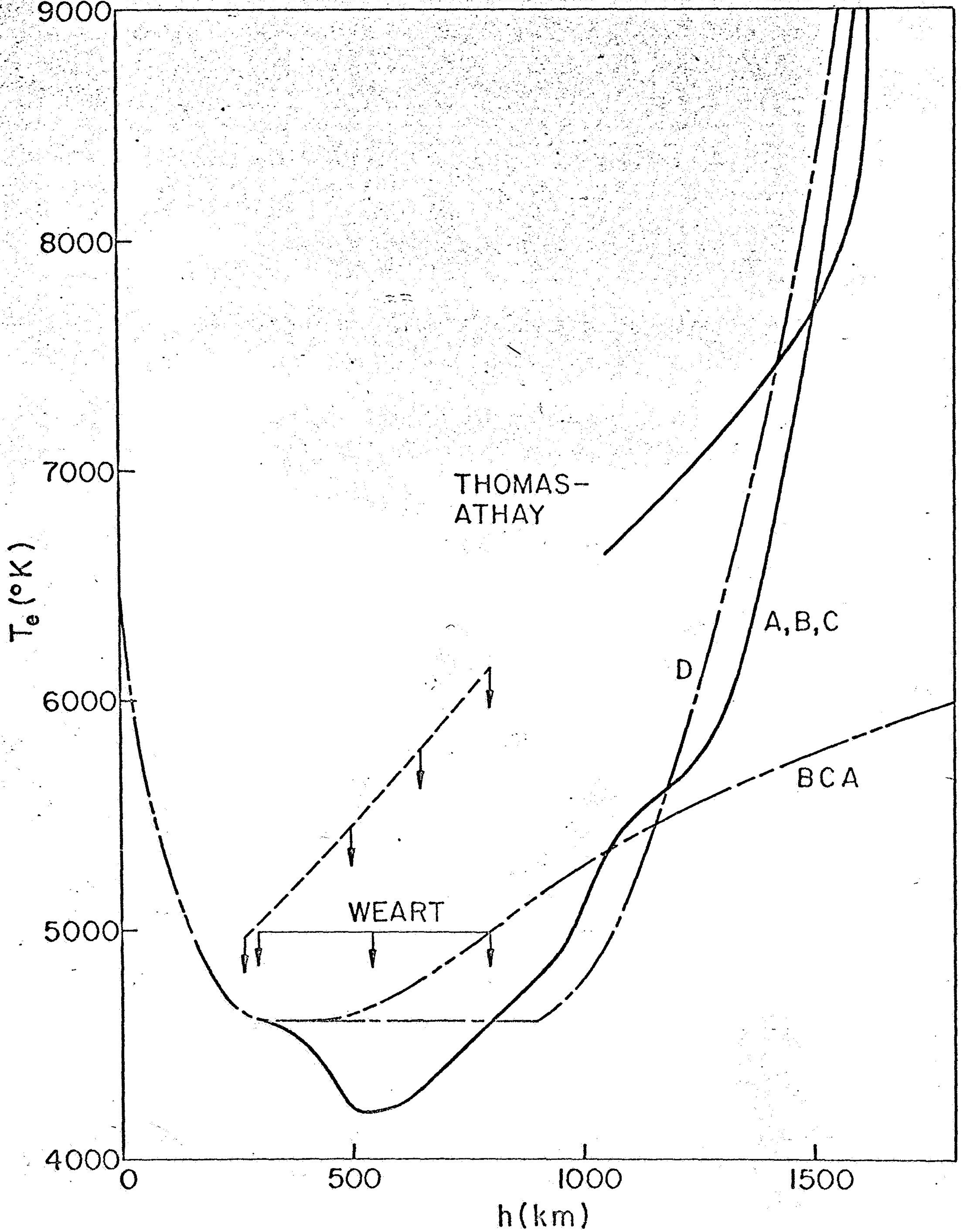
9000
8000
7000
6000
5000
4000
T_e (°K)
0
500
1000
1500
h(km)
THOMAS-
ATHAY
A, B, C
D
BCA
WEART

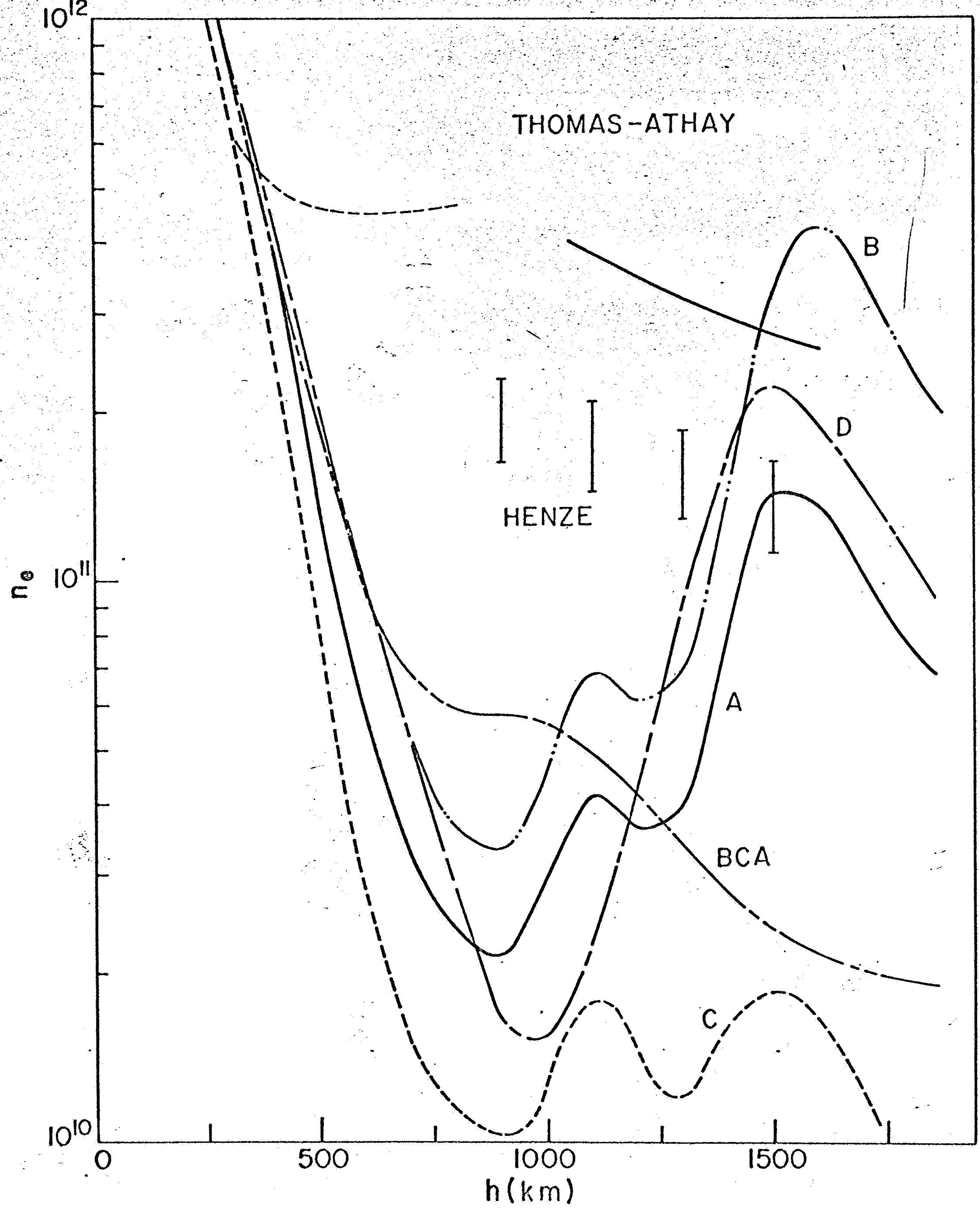

THOMAS-ATHAY
HENZE
B
D
A
BCA
C
10^{12}
10^{11}
10^{10}
n_e
0
500
1000
1500
h(km)

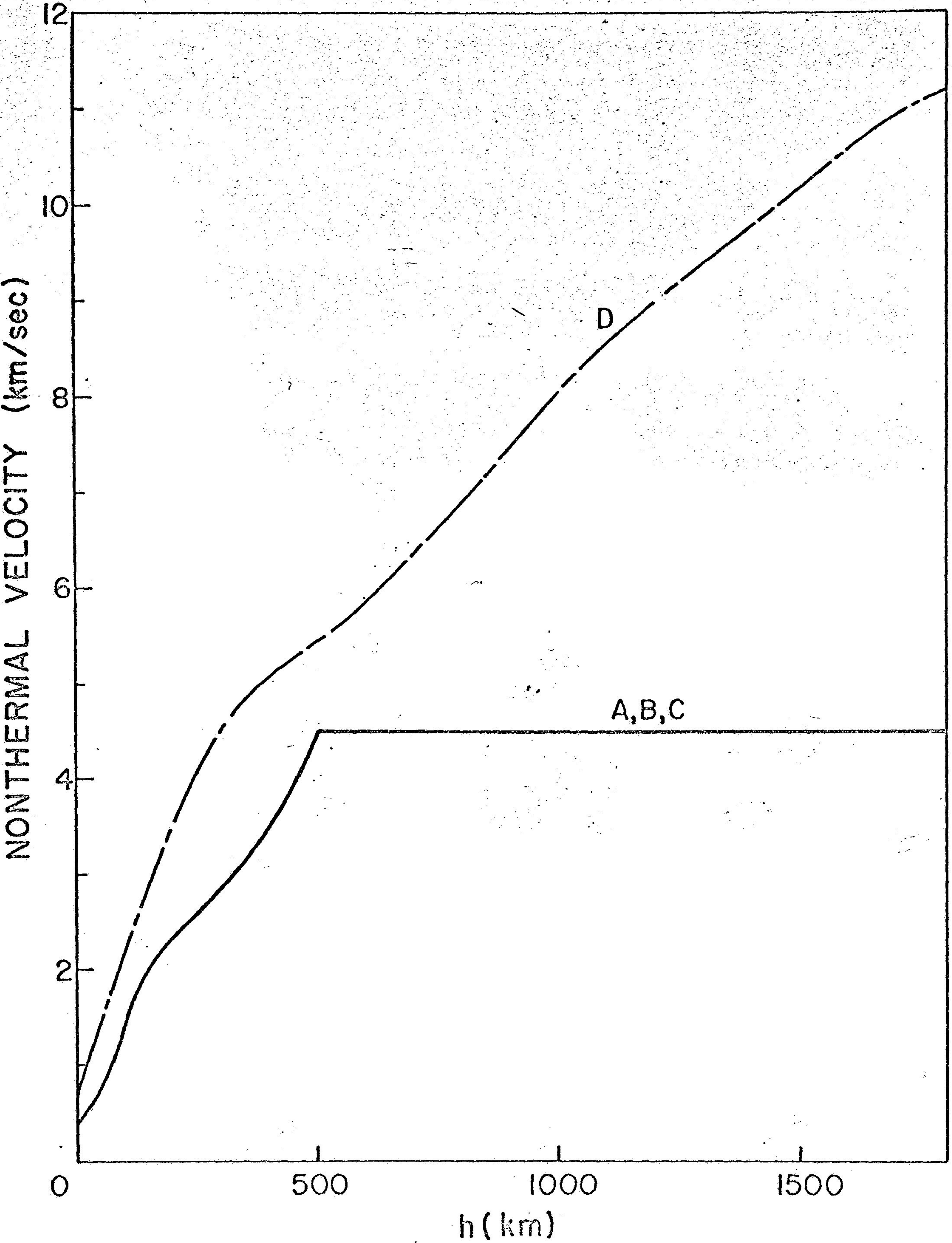

NONTHERMAL VELOCITY (km/sec)
12
10
8
6
4
2
0
500
1000
1500
h (km)
D
A,B,C

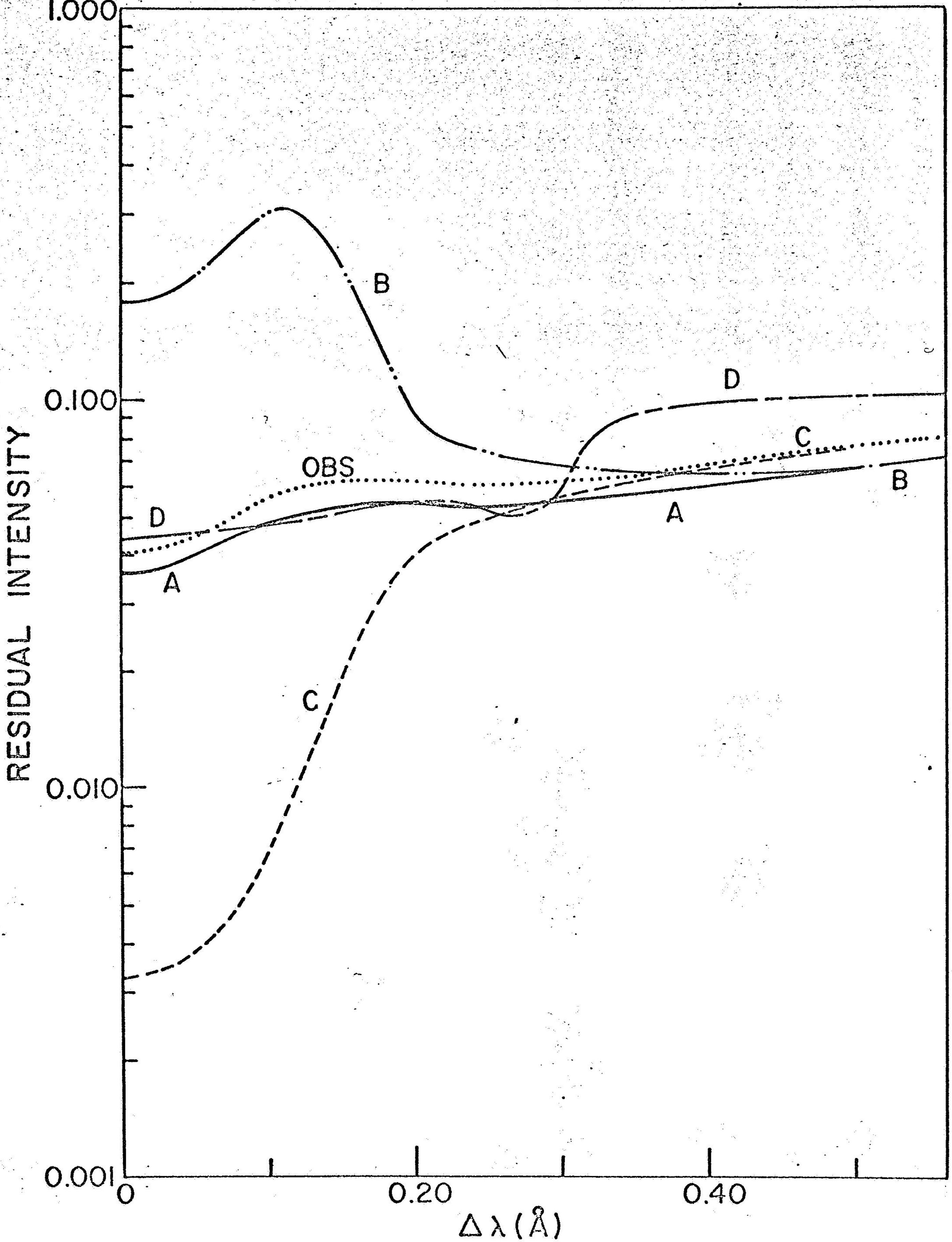

1.000
0.100
0.010
0.001
RESIDUAL INTENSITY
0
0.20
0.40
Δλ (Å)
B
D
C
OBS
D
A
B
A
C

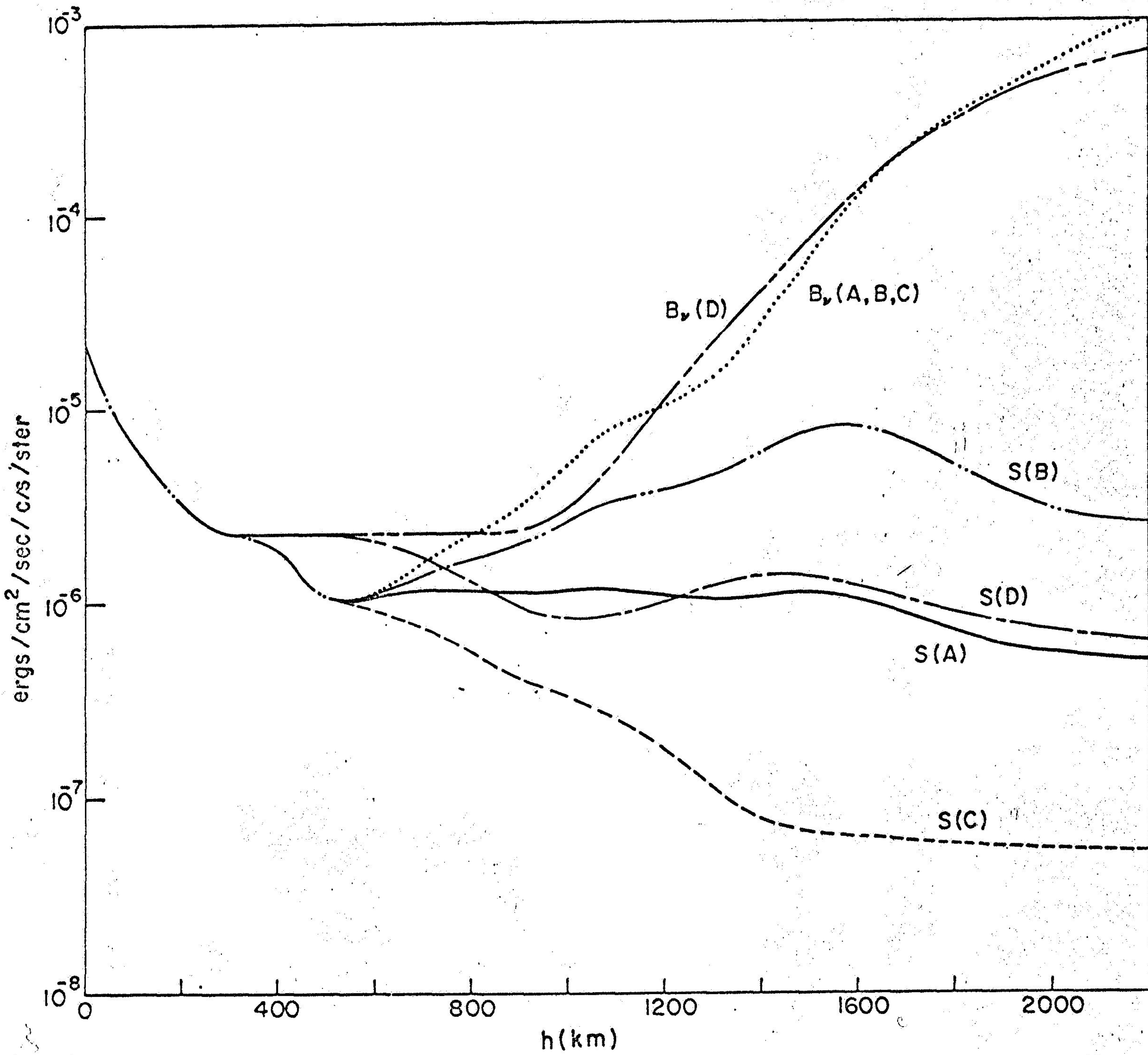

10^{-3}
10^{-4}
10^{-5}
10^{-6}
10^{-7}
10^{-8}
ergs/cm^2/sec/c/s/ster
0
400
800
1200
1600
2000
h(km)
B_ν(D)
B_ν(A,B,C)
S(B)
S(D)
S(A)
S(C)

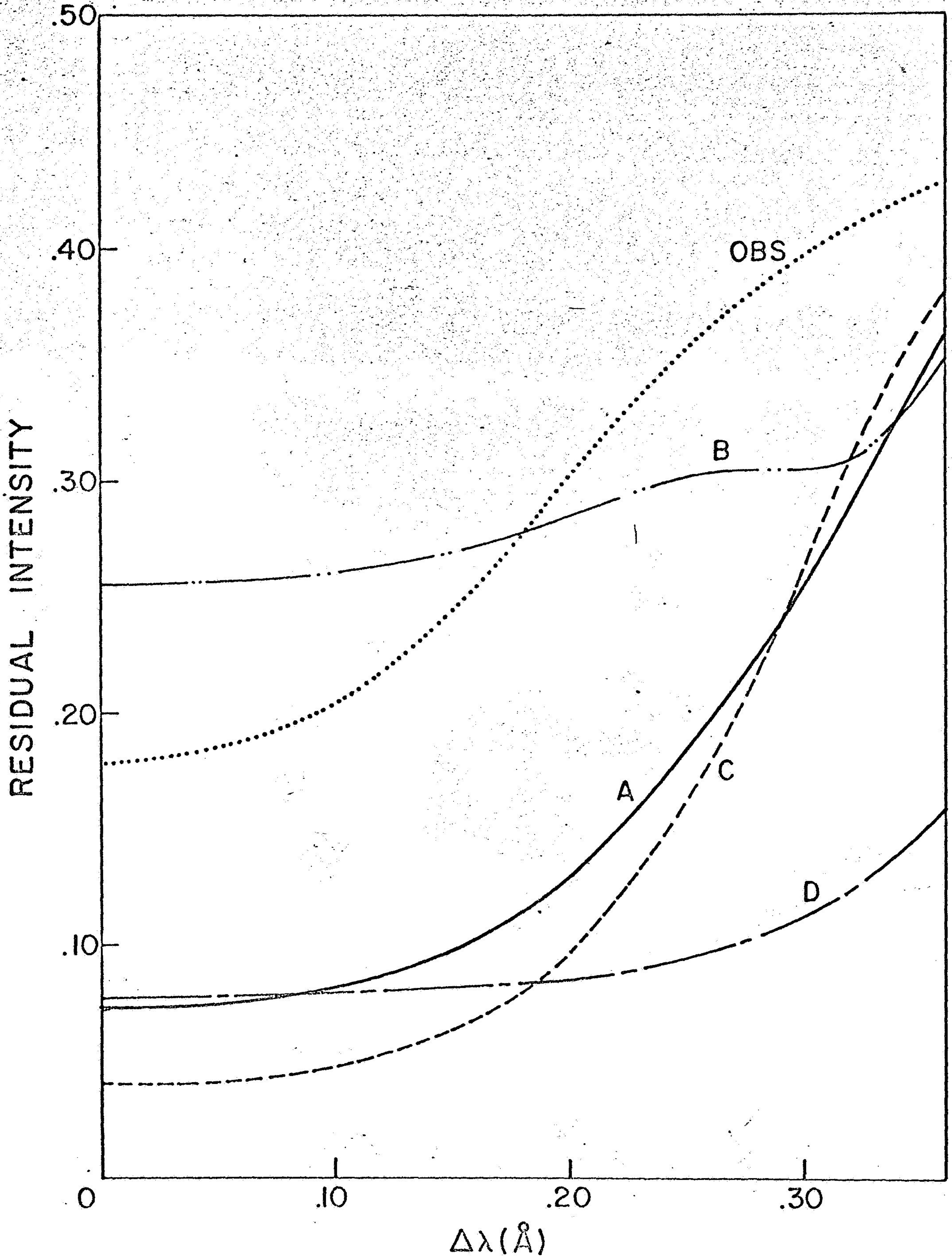
.50
.40
.30
.20
.10
0
.10
.20
.30
RESIDUAL INTENSITY
Δλ(Å)
OBS
B
A
C
D

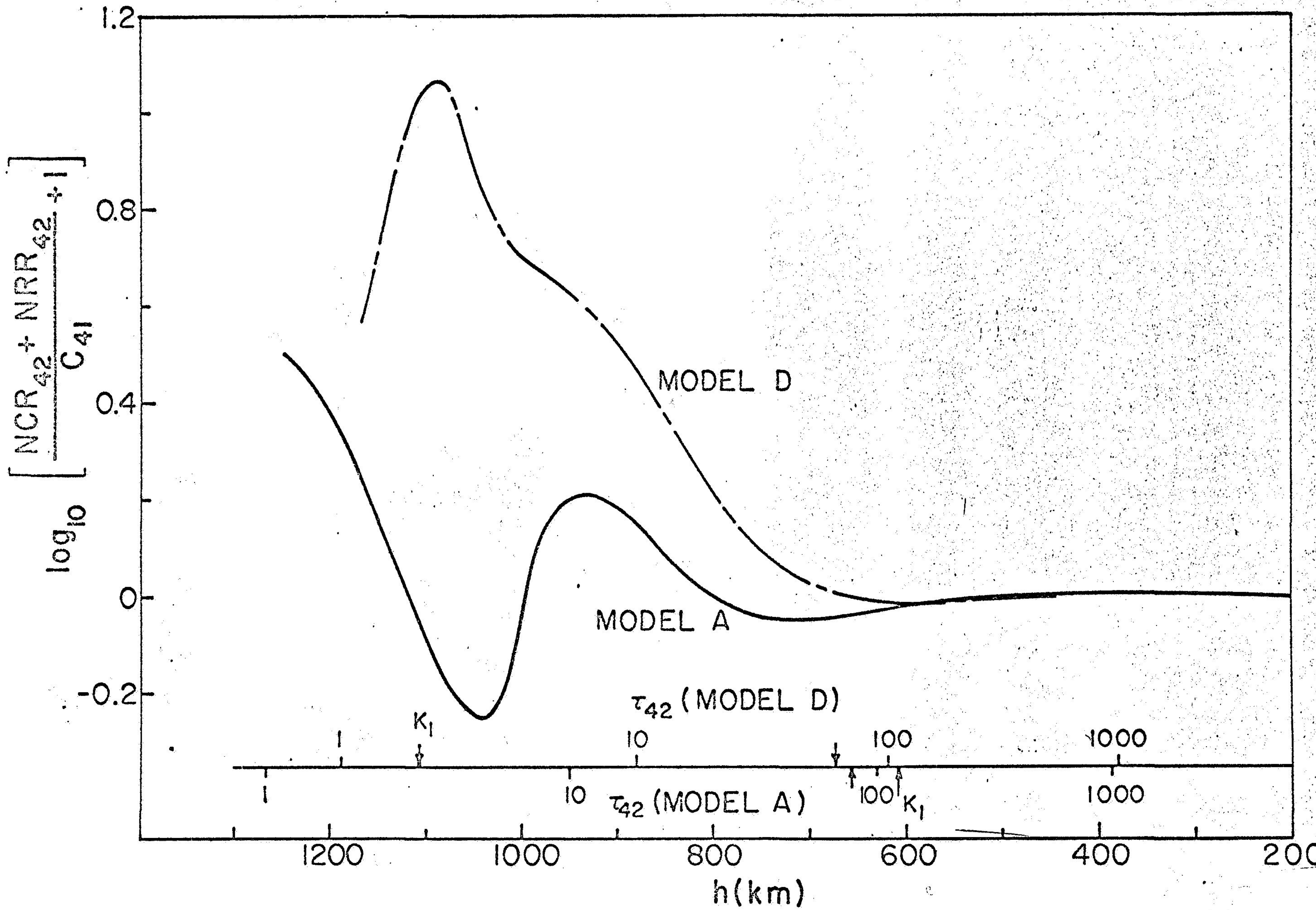

$\log_{10}\left[\frac{NCR_{42}+NRR_{42}}{C_{41}}+1\right]$
1.2
0.8
0.4
0
-0.2
MODEL D
MODEL A
τ_{42} (MODEL D)
1
K_1
10
100
1000
τ_{42} (MODEL A)
1
10
100
K_1
1000
1200
1000
800
600
400
200
h(km)